In *Proceedings of the ANS Topical Meeting on Radiation Protection for our National Priorities, Medicine, the Environment, and the Legacy* (RPS 2000), Spokane, Washington, September 17-21, 2000. *In press*.

TEMPORAL OPTIMIZATION OF RADIOTHERAPY TREATMENT FRACTIONS

Robert D. Stewart, Ph.D.
Radiation and Health Technology
Pacific Northwest National Laboratory
P.O. Box 999, MSIN K3-55
Richland, WA 99352

Richard J. Traub, Ph.D.
Radiation and Health Technology
Pacific Northwest National Laboratory
P.O. Box 999, MSIN K3-55
Richland, WA 99352

ABSTRACT

Intensity-modulated radiation therapy (IMRT) techniques are rapidly becoming the preferred dose delivery method for the treatment of some cancers. IMRT treatments for head and neck cancers typical deliver a total dose of 60 to 70 Gy using dose fractions delivered on 25 to 35 treatment days (about 2 Gy per fraction). To maximize the dose to the tumor while simultaneously minimizing the dose to surrounding normal tissues, 5 or more patient-beam configurations are often used to deliver each dose fraction. Because an irradiator system cannot be moved instantaneously from one patient-beam orientation to another, normal and cancerous cells within a beam experience small pulses of radiation separated by time intervals that range from a few seconds up to as much as 10 to 20 minutes. The total time required to deliver a dose fraction using multiple beam configurations typically ranges from about 10 minutes up to a maximum of 1 or 2 hours. As the time required to deliver a treatment dose increases, cell killing tends to decrease because of damage repair effects. The benefit of using a large number of beam configurations to spare normal tissues needs to be balanced against decreases in tumor-cell killing associated with prolonging the time interval used to deliver the individual dose fractions.

Absorbed dose calculations for 1 MeV, monodirectional photon beams targeted at an idealized neck cancer have been performed using the MCNP computer code. The dose-depth profiles for the individual beams were then used to calculate the cell-killing effects of representative treatment designs using the lethal and potentially lethal (LPL) radiobiological model. Our calculations, which are based on LPL parameter values for colon adenocarcinoma cells, suggest that increasing the time required to deliver each dose fraction from less than a minute up to 1 or 2 hours can decrease the overall cell-killing effects of some treatments by factors as high as 2 to 20. Moreover, dose protraction effects alter the iso-effect treatment dose by factors on the order of 5 to 10%. That is, a 75 Gy treatment produces about the same tumor control probability (TCP) as a 70 Gy treatment if the dose fractions are delivered in 1 to 2 hours instead of a few minutes.

For multi-beam radiation treatments, our studies suggest that it is most likely advantageous to minimize the time required to deliver treatment doses. For broad parallel beams that deliver a relatively uniform dose to the entire tumor, the sequence of beams used to deliver a radiation dose most likely has little affect on treatment outcome. On the other hand, IMRT treatments that use pencil beams of radiation to sequentially target smaller tissue regions can produce very heterogeneous (in time and space) dose distributions, and the sequence of beams used to deliver a treatment dose may be important because of dose protraction effects associated with damage repair.

I. INTRODUCTION

Monte Carlo transport calculations in patient-specific anatomical (voxel) constructs derived from CT and MRI scans represent the current state-of-the-art in dosimetry for radiation treatment planning purposes. Monte Carlo dosimetry systems such as these are capable of estimating depth-dose profiles for clinical accelerators to an accuracy of about 1 to 3% [Ma99]. Moreover, computer automated techniques to shape the dose delivered to a region of tissue using intensity-modulated radiation therapies (IMRTs) are a main focus of current research. Computer-automated IMRT methods provide many new opportunities to escalate the dose delivered to a tumor without a concomitant increase in the dose to the surrounding normal tissues. However, IMRT techniques often produce a more heterogeneous dose distribution, in both time and space, than more traditional irradiation technologies, and the radiobiological consequences of new dose delivery methods and altered fractionation schedules are still largely unknown [Pu99].

IMRT treatments for head and neck cancers typical deliver a total dose of about 60 to 70 Gy using dose fractions delivered on 25 to 35 treatment days (about 2 Gy per fraction). To maximize the dose to the tumor while simultaneously minimizing the dose to surrounding normal tissues, 5 or more beam configurations are often used to deliver each dose fraction. Moreover, multi-leaf collimators are used to shape each beam of radiation to the contours of different tissue regions. For example, one leaf configuration might shape the radiation beam to the contours of a visibly diseased region of tissue, and a second leaf configuration might shape the beam to target tissue at risk for microscopic (subclinical) disease. Because an irradiator system cannot be moved instantaneously from one leaf or beam configuration to another, treated cells experience small "pulses" of radiation separated by time intervals that range from a few seconds up to as much as 10 to 20 minutes. The total time required to deliver a dose fraction using multiple beam orientations typically ranges from about 10 minutes up to a maximum of about 2 hours.

The so-called four Rs of radiation therapy are repair effects, reoxygenation effects, cell-cycle redistribution (or resensitization) effects, and repopulation effects. As the time between pulses of radiation increases, reoxygenation and cell-cycle redistribution effects tend to increase cell killing, and repair and repopulation effects tend to decrease cell killing. Figure 1 shows an idealized schematic illustrating trends in cell killing associated with these processes. To fully exploit the potential of radiation therapy, treatment designs must carefully balance increases in cell killing associated with the minimization of tumor-cell repair and repopulation effects against decreases in cell killing associated with reoxygenation and cell-cycle redistribution effects. However, the time constants associated with damage repair effects are typically on the order of a few minutes to an hour or two whereas redistribution, reoxygenation, and repopulation effects are most likely only important when pulses of radiation are separated in time by a few hours to a few days. For the series of 5 to 15 radiation pulses typically experienced by a tumor during the delivery of a dose fraction, damage repair is most likely the main biophysical process affecting tumor-cell killing.

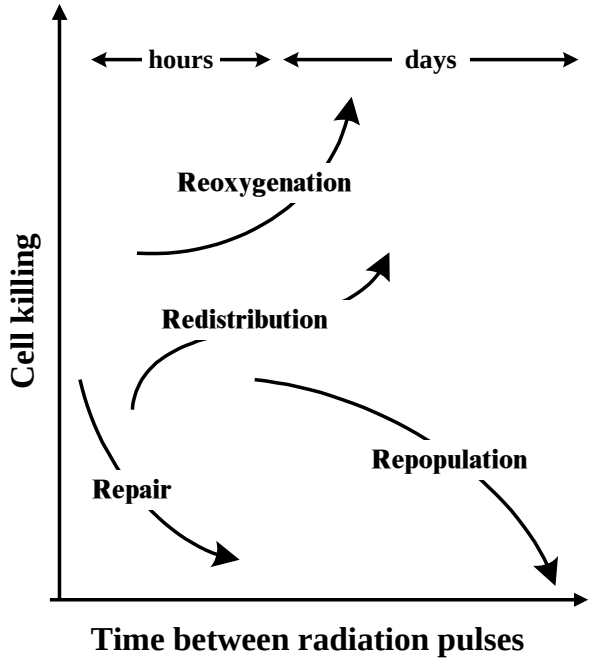

Figure 1. An idealized schematic illustrating trends in cell killing associated with repair effects, cell-cycle redistribution effects, reoxygenation effects, and repopulation effects. The relative importance of the four effects are not drawn to scale.

Because each beam configuration produces a unique absorbed dose distribution in the tumor (and the surrounding normal tissues), different sequences of radiation beams may produce different treatment outcomes. That is, it may be possible to modulate the timing or sequence of radiation beams used to deliver a treatment dose in a way that increases the tumor control probability (TCP). In this work, the relative importance of beam sequence and dose protraction (damage repair) effects on tumor-cell killing are examined. We also examine possible ways to exploit these effects to improve the outcome of representative radiation treatments for head and neck cancers.

II. METHODOLOGY

For the present study, the idealized neck tumor shown in Figure 2 is used to investigate the effects on cell killing and the TCP of protracting the dose-fraction delivery time and, also, the sequence of beams used to deliver treatment doses. First, the volume of a tumor is sub-divided into 2,328 smaller tissue regions (i.e., voxels), and the MCNP Monte Carlo radiation transport code [Br97] is used to calculate the absorbed dose delivered to each voxel by eight different beam configurations. That is, monodirectional photon beams are directed at the center of the tumor from 8 different directions as indicated in Figure 2. Next, an absorbed dose rate "history" function, $\dot{D}(t)$, is constructed for each voxel from the MCNP-calculated absorbed dose distribution. The total treatment dose, *D*, is the integral of $\dot{D}(t)$ over all time. The relative intensity of the beams are normalized so that the absorbed dose delivered to a target voxel located near the center of the tumor equals a prescribed value, as recommended by the International Commission on Radiation Units and Measurements (ICRU) [IC93]. Finally, the number of viable tumor cells remaining in each voxel after the treatment, as well as a probability of tumor control, is calculated using our Kinetic Biological Effects Modeling (KBEM) software. Additional details on the TCP calculations are provided below.

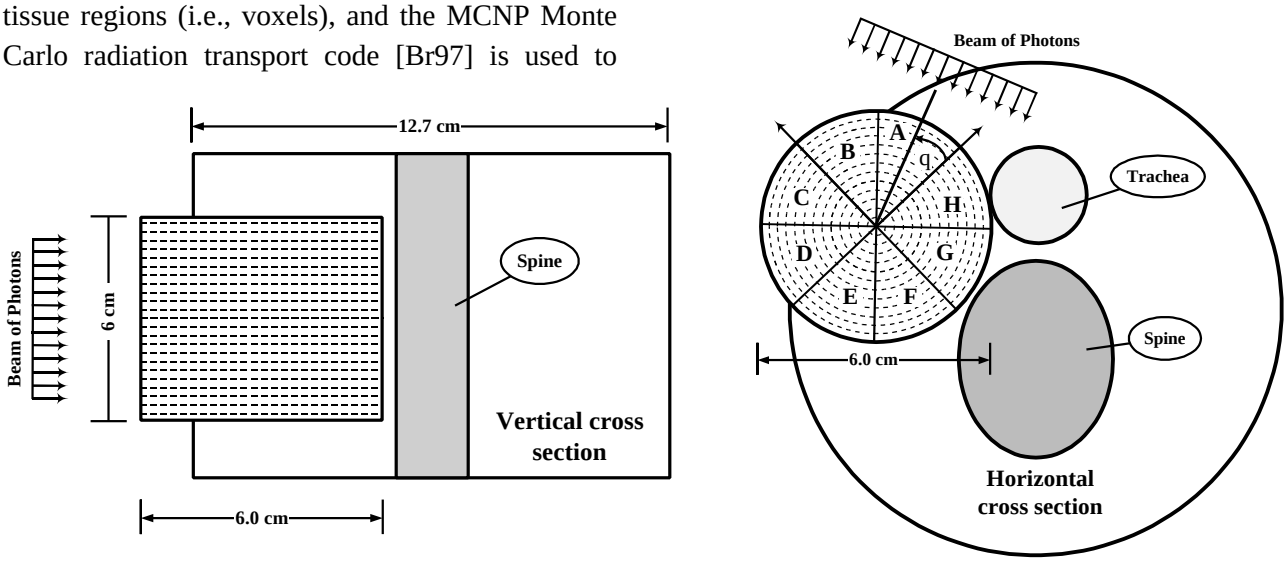

Figure 2. Schematic of an idealized tumor located in the neck. The tumor is modeled as a right circular cylinder 4.6 cm high with a diameter of 4.5 cm (i.e., the gross tumor volume [IC93]). The tumor cells are surround by a small layer of tissue at risk for subclinical disease. Elemental compositions and densities for the tumor (1.04 g cm^{-3}), soft tissue of the neck (1.04 g cm^{-3}), and spine (1.4 g cm^{-3}) are from [Cr87]. The physical dimensions of the neck, trachea, and spine are adapted from [IC92]. Tumor control probabilities are calculated for a region of tissue that contains 6.9×10^{10} tumor cells uniformly distributed within a 69 cm^3 tissue volume (i.e., a cell density of 10^9 cells cm^{-3}). Tumor cells located in the region of tissue at risk for sub-clinical disease are not included in the TCP estimates. An example MCNP input file and other details of the calculations are available on-line at http://www.pnl.gov/berc/epub/pnnl33246/

Radiobiological Modeling in Voxel Constructs

The Pacific Northwest National Laboratory (PNNL) has developed software to perform radiobiological simulations in voxel constructs using either the lethal and potential lethal (LPL) model [Cu86] or the repair-misrepair (RMR) model [To85]. A more sophisticated version of this software package, based on a multi-lesion kinetic model [St00], that can be used to account for cycle-cycle redistribution and repopulation effects is under development (see http://www.pnl.gov/berc). In both the LPL and RMR models, radiation-induced DNA damages are created at a rate proportional to $\dot{D}(t)$ and then repaired correctly or misrepaired to form a fatal lesion.

The expected fraction of cells surviving a treatment that delivers dose D is calculated from $S(D) = \exp[-L_f(D)]$ [Cu86]. Here, $L_f(D)$ denotes the expected number of fatal lesions produced, per cell, a long time after the irradiation ends. The KBEM software uses Visual Numeric's ISML® DIVPAG routine to integrate the system of differential equations used in the LPL and RMR models forward in time using Gear's backward differentiation algorithm [Ge71, Sh79] for an arbitrarily complex dose-rate function $\dot{D}(t)$. Analytical and numerical (KBEM-based) solutions for the LPL and RMR models agree to better than six significant digits for a wide range of absorbed dose and dose-rate exposure conditions.

A user application, called VOXEL, based on the KBEM software has been created to calculate the expected number of viable cells produced in a tissue that has been sub-divided into an arbitrary number of voxels. The VOXEL application imports an absorbed dose distribution, constructs a dose-rate history function $\dot{D}(t)$ for each voxel, and then sequentially executes the LPL or RMR model for each voxel to compute the fraction of cells that survive a treatment. Then, a tumor control probability is computed using the formula [We93, Eb96]

$$\mathrm{TCP} = \exp\left\{-\sum_{i=1}^{Q} N_i S_i(D)\right\}, \qquad (1)$$

where N_i is the initial (pre-treatment) number of tumor cells in the ith voxel and $S_i(D)$ is the fraction of the tumor cells in the ith voxel that survive a treatment that delivers absorbed dose D. For the present work, all cell survival calculations are performed using the LPL model and a parameter set (h_{PL} = 3.01 Gy^{-1} cell^{-1}, h_L = 0.192 Gy^{-1} cell^{-1}, e_{PL} = 0.347 h^{-1}, e_{2PL} = 6.74 × 10^{-3} h^{-1}) that yields surviving fractions consistent with the linear-quadratic (LQ) model parameters reported by Deschavanne *et al.* [De90] for DLD1a colon adenocarcinoma cells irradiated by low-LET radiation. A reasonable estimate of the number of tumor cells in the ith voxel, N_i, is obtained by multiplying the volume of each voxel by a representative cell density. For a typical tumor, cell densities on the order of about 10^9 cells cm^{-3} are expected.

III. RESULTS

As a first step towards examining the possible clinical significance of protracted dose fraction delivery times (1 to 2 hours to deliver a dose fraction instead of a few seconds), we first examine the cell-killing effects of several treatment designs in a 1-voxel tissue construct. The results shown in Table 1 indicate that the compounded effects of delivering each of 30 treatment doses in 1 or 2 hours instead of "instantaneously" may reduce the tumor-cell killing effects of a treatment by factors as high as 2 to 20.

To further investigate the possible clinical significance of these dose protraction effects, the idealized neck tumor shown in Figure 2 was used to compute tumor control probabilities for several, 8-

Table 1. The fraction of tumor cells surviving a 30 day treatment delivered using 10 radiation beams of equal intensity. Each beam configuration delivers a pulse of radiation (0.1 to 0.2 Gy) to the tumor cells at 1000 Gy h^{-1}. Dose-fraction delivery times of 60 minutes and 120 minutes correspond to beam reconfiguration times of 6.67 and 13.3 minutes, respectively.

Total dose (Gy)	**Dose per fraction (Gy)**	**Surviving fraction for several dose fraction delivery times**			**Ratio of protracted to acute**	
		0 min.	**60 min.**	**120 min.**	**60 min.**	**120 min.**
35.0	1.167	3.904E-05	5.563E-05	8.582E-05	1.42	2.20
40.0	1.333	5.364E-06	8.483E-06	1.487E-05	1.58	2.77
45.0	1.500	6.495E-07	1.154E-06	2.334E-06	1.78	3.59
50.0	1.667	6.946E-08	1.403E-07	3.323E-07	2.02	4.78
55.0	1.833	6.575E-09	1.528E-08	4.299E-08	2.32	6.54
60.0	2.000	5.521E-10	1.493E-09	5.061E-09	2.70	9.17
65.0	2.167	4.122E-11	1.311E-10	5.429E-10	3.18	13.17
70.0	2.333	2.741E-12	1.037E-11	5.315E-11	3.78	19.39

beam treatments. Figure 3 summarizes the TCP values obtained for treatments that deliver a range of total doses sub-divided into 30 dose fractions (2 to 2.8 Gy per fraction). Treatment doses are delivered once per day, at the same time of day, for 39 consecutive days (treatment doses are only delivered on weekdays). The solid lines indicate the TCP values based on the MCNP-calculated absorbed dose distributions with beam sequence ABCDEFGH (i.e., Beam A followed by Beam B followed by Beam C and so on).

Calculations are shown in Figure 3 for dose fractions delivered very rapidly (each beam pulse is delivered at 1000 Gy h^{-1} and the irradiator system moves instantaneously between orientations), 23 minutes, 42 minutes, 63 minutes, and 105 minutes. Dose fraction delivery times of 23, 42, 63, and 105 minutes correspond to beam re-orientation times of 3, 6, 9, and 15 minutes (e.g., 3 minutes to move from orientation A to B). The prescribed treatment dose is based on a target voxel located in the center of the tumor at z = 4.5 cm (z = 0 is the bottom of the tumor; refer to Figure 2). To help quantify the importance of dose heterogeneities within the tumor volume, TCP values are also shown (circles) for the special case when each voxel in the tumor experiences exactly the same (prescribed) dose, i.e., the rate history function $\dot{D}(t)$ is the same for all

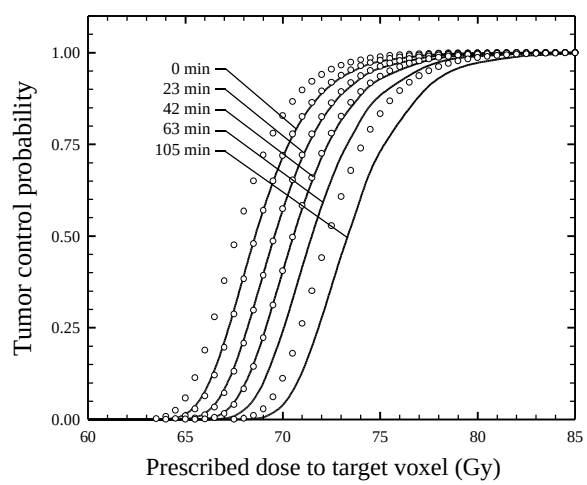

Figure 3. Effect on the TCP of increasing the dose-fraction delivery time from a few seconds up to 105 minutes. Solid lines indicate TCP values based on the MCNP-calculated absorbed dose distribution. Circles indicate TCP values calculated for the special case when all regions of the tumor experience exactly the same (prescribed) treatment dose.

voxels.

The data shown in Figure 3 clearly demonstrate that damage repair effects associated with increasing dose delivery times from a few seconds up to 105 minutes (1.75 h) significantly decreases the predicted TCP values. For example, to obtain a TCP value of 0.75 (75% probability no tumor cells survive the treatment), the prescribed treatment dose must be increased from 70 Gy to 75 Gy if dose fractions are delivered in 105 minutes (15 minutes to move between orientations) instead of a few seconds. Even for the shorter dose fraction delivery times of 23 or 42 minutes, the predicted TCP values are noticeably different than the TCP values calculated when each dose fraction is delivered in a few seconds. Comparison of TCP values for the MCNP-calculated and completely uniform dose distribution suggest that dose heterogeneities within the tumor volume (the minimum dose recorded in a voxel was about 24% lower than the maximum recorded dose) tend to shift the TCP curve to higher prescribed doses. The shape of the TCP curve, however, does not appear to be affected by dose heterogeneities.

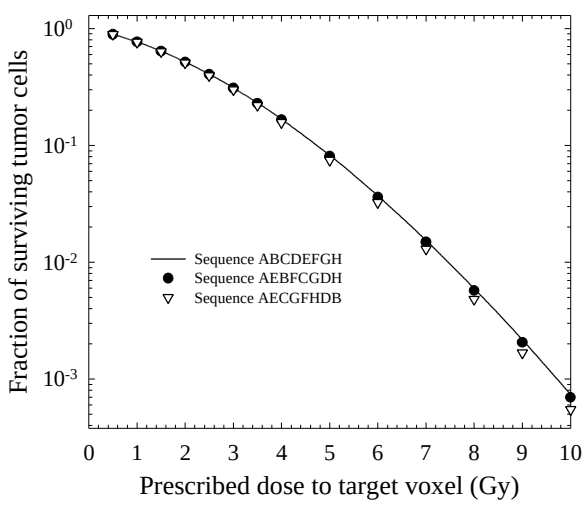

Figure 4. Effect on cell survival of altering the sequence of beams used to deliver a single treatment fraction. The dose fraction is delivered as a series of 8 intensity-modulated radiation pulses separated by a 15 minute time interval (i.e., it takes 15 minutes to move the irradiator system from one orientation to the next).

Because each beam configuration produces a different absorbed dose distribution in the tumor, it is possible that the tumor-cell killing effects of a treatment can be modulated by altering the sequence of beams used to deliver the dose fractions. To examine this possibility, the fraction of cells surviving treatment doses from 0.5 to 10 Gy were calculated for three different beam sequences (refer to Figure 2): ABCDEFGH, AEBFCGDH, and AECGFHDB. When equal beam intensities are used (each beam delivers 12.5% of the prescribed dose to the target voxel), the TCP values and fraction of tumor cells surviving a treatment are the same to about 5 or 6 significant digits for all three beam sequences. If the intensity of beam A, C, E, and G are increased ten-fold relative to beams B, D, F, and H (an intensity-modulated treatment design), some small differences in tumor-cell killing effects are predicted at higher doses (Figure 4). For the broad parallel beams used in the present study, the sequence of beams used to deliver a dose fraction most likely have only a small affect on treatment outcome.

IV. CONCLUSIONS

Because of damage repair (dose protraction) effects, cell killing tends to decrease as the time required to deliver a dose fraction increases. Our calculations suggest that increasing the time required to deliver a dose fraction from a few seconds up to 1 or 2 hours can decrease the overall cell-killing effects of some treatments by factors as high as 2 to 20. Also, calculations suggest that dose protraction effects alter the iso-effect treatment dose by factors on the order of 5 to 10%. That is, a 75 Gy treatment produces about the same tumor control probability (TCP) as a 70 Gy treatment if the dose fractions are delivered in 1 to 2

hours instead of a few minutes. Even for dose fraction delivery times as short as 20 to 30 minutes, tumor control probabilities may be noticeably affected by damage repair. To maximize the effectiveness of radiation treatments, it is most likely advantageous to minimize dose fraction delivery times. For the broad parallel beams used in the present study, the sequence of beam configurations used to deliver a dose fraction most likely has a small effect on treatment outcome. However, IMRT treatments that use pencil beams of radiation to sequentially target smaller regions of tissue (e.g., sequential target portions of the gross tumor volume) can produce very heterogeneous (in time and space) dose distributions, and the sequence of beams used to deliver treatment doses could be important.

ACKNOWLEDGEMENTS

Work supported by the U.S. Department of Energy under contract DE-AC06-76RLO 1830.

REFERENCES

[Br97] JF Briesmeister, Editor, MCNP – A General Monte Carlo N-Particle Transport Code. Los Alamos National Laboratory Report, LA-12625-M (March, 1997).

[Cr87] M Cristy and KF Eckerman. *Specific Absorbed Fractions of Energy at Various Ages from Internal Photon Sources. I. Methods*. ORNL/TM-8381/V1. Oak Ridge National Laboratory, Oak Ridge, TN 37831 (1987).

[Cu86] SB Curtis, Lethal and potentially lethal lesions induced by radiation – A unified repair model, *Radiat. Res.* **106**, 252-270 (1986). See also S.B. Curtis, Erratum. *Radiat. Res.*, **119**, 584 (1989).

[De90] PJ Deschavanne, B Fertil, N Chavaudra, and EP Malaise, The Relationship between Radiosensitivity and Repair of Potentially Lethal Damage in Human Tumor Cell Lines with Implications for Radioresponsiveness. *Radiat. Res.* **122**(1), 29-37 (1990).

[Eb96] MA Ebert and PW Hoban, Some characteristics of tumour control probability for heterogeneous tumours. *Phys. Med. Biol.*, 41(10), 2125-2133 (1996).

[Ge71] CW Gear, Chapter 11 in *Numerical Initial Value Problems in Ordinary Differential Equations*, Prentice-Hall, Englewood Cliffs, New Jersey 1971.

[IC92] ICRU. Phantoms and Computational Models in Therapy, Diagnosis and Protection, Report 48. International Commission on Radiation Units and Measurements. Bethesda, Maryland (1992).

[IC93] ICRU. Prescribing, Recording, and Reporting Photon Beam Therapy, Report 50. International Commission on Radiation Units and Measurements. Bethesda, Maryland (1993).

[Ma99] CM Ma, E Mok, A Kapur, T Pawlicki, D Findley, S Brain, K Forster, AL Boyer, Clinical implementation of a Monte Carlo treatment planning system. *Med. Phys.*, **26**(10), 2133-2143 (1999).

[Sh79] LF Shampine and C.W. Gear, A user's view of solving stiff ordinary differential equations. *SIAM Review* **21**,1-17 (1979).

[St00] RD Stewart, JK Shultis, and BA Montelone, A Kinetic Biological Effects Model for Quiescent Cells. Pacific Northwest National Laboratory Report PNNL-13258, Richland, WA 99352, May 30 2000. Available on-line at http://www.pnl.gov/berc/epub/pnnl13258/

[To85] CA Tobias, The repair-misrepair model in radiobiology: Comparison to other models, *Radiat. Res. Suppl.* **104**, 77-95 (1985).

[We93] S Webb and AE Nahum, A model for calculating tumour control probabilities in radiotherapy including the effects of inhomogeneous distributions of dose and clonogenic cell density. *Phys. Med. Biol.*, **38**, 653-666 (1993).